

ORIGINAL ARTICLE OPEN ACCESS

Surface Characterization of Skin Substitute Materials

Alexander Jaekel  | Michaela Wirtz

Department of Natural Sciences, University of applied Sciences Bonn-Rhein-Sieg, Rheinbach, Germany

Correspondence: Michaela Wirtz (michaela.wirtz@h-brs.de)

Received: 7 November 2024 | Revised: 30 April 2025 | Accepted: 20 May 2025

Funding: This research was supported by the German Federal Ministry of Education and Research (BMBF) (grant number 13FH022KX1).

Keywords: Cutometer | in vitro | IR spectroscopy | microscopy | roughness | skin substitute | skin surface

ABSTRACT

Background: Transdermal therapeutic systems use substance transport through the skin to provide an active pharmaceutical ingredient. To ensure a reliable supply, adhesion to skin must be guaranteed. In practice in vivo studies as well as in vitro studies on steel (ISO-standard for self-adhesive tapes) are used. As in vitro—in vivo correlation is poor, extensive in vivo studies are applied during industrial product performance tests. Hence, a specialized skin substitute material for in vitro adhesion testing is needed.

Materials and Methods: Synthetic leather (polyurethane), silicone (Dragon Skin), gelatines, and VitroSkin are used as skin substitute materials. For topographical analysis, reflected light microscopy and confocal light microscopy are applied. Infrared spectroscopy is performed for analysis of functional groups. Dermatological skin probe systems are used to analyze friction, surface pH, and elasticity. To bundle all data with regards to skin similarity, mid-level data fusion is applied.

Results: For all substitute materials, common topographic characteristics compared to human skin can be observed. However, all materials show limitations regarding their topography. Gelatine and VitroSkin feature comparable surface functionality compared to human skin. All materials show significant deficits in their mechanical properties. All characteristics can be summarized as the Skin Similarity Index to give a comprehensive overview regarding substitutes similarity to skin.

Conclusions: A comprehensive evaluation of topography, chemical functionality, and mechanical properties regarding a skin substitutes similarity to human skin was performed. This data should be considered as a baseline for further research in the field of adhesion to skin. By adding further characteristics and materials, it is a versatile approach that can be implemented in a variety of areas.

1 | Introduction

The skin is the largest organ in the human body by surface area [1] and its outermost layer. As such, it is a protector from the environment and a regulating factor in the modulation of body temperature as well as water loss [2, 3]. As the regulation of water loss suggests, the human skin is a permeable organ. Substance transport through the skin is possible and hereto commonly utilized for so-called transdermal therapeutic systems (TTS). These systems adhere to the skin surface for several days [4] and are meant to provide a continuous delivery

of low-dose active pharmaceutical ingredient (API) into the organism [5].

Due to their pharmaceutical use, TTS need to be safe, therapeutically efficient, and of consistent quality. As the API is the biggest impact factor regarding those attributes, clinical studies target primarily medical aspects of TTS but only marginally touch upon the system's adhesive properties [1]. For adhesion, testing procedures for self-adhesive tapes are applied according to ISO 29862:2018 [6] and ISO 29863:2018 [7]. These norms dictate the testing of adhesion to skin by adhesion to steel. From experience,

This is an open access article under the terms of the [Creative Commons Attribution-NonCommercial-NoDeriv](https://creativecommons.org/licenses/by-nc-nd/4.0/) License, which permits use and distribution in any medium, provided the original work is properly cited, the use is non-commercial and no modifications or adaptations are made.

© 2025 The Author(s). *Skin Research and Technology* published by John Wiley & Sons Ltd.

despite *in vitro* tests with steel, extensive human wear studies are necessary to ensure adequate adhesion without issues during the removal. However, human studies are not encouraged due to ethical reasons and the associated temporal and financial expenses. To minimize human testing, an *in vitro* adhesion test for TTS and adhesive patches, in general, is urgently needed, for which a skin substitute is an alternative to human skin.

In the literature, a wide variety of human skin substitute materials for different applications are described. Most often mentioned are skin grafts from human reconstructed skin that are primarily used for skin transplantation surgery in emergency medicine. However, these substitutes are inapplicable for *in vitro* adhesion to skin testing, as they are extraordinarily expensive and mostly have an insufficient shelf-life [8–18]. In contrast, such skin substitutes are common in drug permeation tests [19–23] and are used for skin irritation testing and toxicological evaluation of topically applied drugs [19]. In addition to these substitutes, less costly materials that are not readily available for medicine are actively researched [24, 25].

Another less costly and already commercially available skin substitute is VitroSkin, which is a collagen-based membrane. It claims to mimic pH, critical surface tension, ionic strength, chemical reactivity, and topography of human skin. It mainly serves UV protectant testing [26] and is studied in scientific literature, too. It was found to have surface functionalities, surface tension parameters, adhesive force, and coefficient of friction comparable to mammalian skin, whereas its topography was found to differ significantly [27, 28].

For skin topography replication, the literature suggests the use of a molding approach by applying Dragon Skin, a silicone typically used in the make-up design. However, it was found to differ from human skin regarding functionality and contact-angle [28].

Such molding used with Dragon Skin is applicable to other materials as well, including gelatine mixtures used in make-up design or those specifically designed to mimic human skin [27, 29–33]. Lir et al. introduced a specifically modified gelatine mimicking surface structure, mechanical properties, contact angles, wettability, adhesive force, and coefficient of friction of skin [27, 33] as a promising alternative to previous approaches using gelatine. Less specific, yet often used for industrial adhesion testing due to its availability, chemical functionality, and structure, is synthetic leather from polyurethane (PU).

In addition to the materials mentioned above are cellulose acetate and collagen, commonly known as skin substitute materials [1, 9, 11, 30, 31, 33]. However, cellulose acetate is primarily used to replicate skin for scanning electron microscopy [33], and collagen is extraordinarily complex in crosslinking and shaping/molding into a skin-like membrane [34–39]. Therefore, these materials are not studied in this work.

Despite the numerous approaches to skin substitutes, lack of comparability and incomplete characterizations provide the pressing need for further investigation. Therefore, the aim of this study is to characterize structural surface properties, as well as mechanical and chemical properties of the above-mentioned materials. The goal is to build the foundation for future research on *in vitro*

adhesion-to-skin testing for adhesive patch systems, especially TTS, by implementation of a “Skin Similarity Index” for all described materials.

2 | Material and Methods

2.1 | Materials

To simulate skin, gelatine 180 bloom, 37% formaldehyde, ethanol, and glycerol (Carl Roth, Germany) are used. Additionally, Dragon Skin 20 is purchased from KauPo Plankenhorn, Germany. Furthermore, Silflo (Monaderm, France) is used to manufacture skin molds. Other readily available materials used as skin substitutes are: Gelafix (Kryolan, Germany), synthetic leather (grey) based on polyurethane covered polyamide (DuPont, France), and VitroSkin (Florida Suncare Testing Inc., USA). For surface characterization, two different microscopes are used, the first being a reflected light microscope (LM) VHX-7100 from Keyence (Japan) and the second being a confocal light microscope (CLM) MarSurf CM explorer from Mahr (Germany). The objectives used are VHX-E20, VHX-E100, and VHX-E500 (Keyence, Japan) for the LM and Optikmodul 1600S, Optikmodul 800S, Optikmodul 320S and Optikmodul 160S (Zeiss, Germany) for the CLM. To analyze the functional groups, a Nicolet iS50 ATR with a diamond attenuated total reflectance (ATR) crystal (Thermo Fisher Scientific, USA, Massachusetts) is used. For dermatological analysis, Cutometer dual MPA 580, MPA 2, Ambient Condition Sensor RHT 400, Skin-pH-Meter pH 905, Frictiometer FR 700 and Cutometer Dual MPA 580 (2 mm) (Courage + Khazaka electronic, Germany). Software-wise, Microsoft Excel, OriginLab Pro 2021 (academic), Omnic version 9.12.928, MarSurf metrology SW version 8.8, MPA CTplus version 1.1.5.0, and VHX Control System version 18.12.04.0A are used.

2.2 | Creation of Skin Substitutes

Not all skin substitute materials are ready for use. VitroSkin needs to be prepared according to its rehydration protocol [40]. All other prepared skin substitutes use a molding approach utilizing a silicone skin imprint (Silflo [41]) of the posterior shoulder of a young male individual. Subsequently, Dragon Skin is poured into the imprint using a commercially available skin moisturizer as a mold release. Inside the mold, Dragon skin is left to cure according to the manufacturer’s instructions [42]. Deviating from the instructions, Dragon Skin is degassed in *vacuo* for 15 min beforehand [28]. Similarly, Gelafix is prepared according to its instruction manual [29].

Lastly, modified gelatine is cured in an above described mold as well, following its preparation according to the workflow of Lir et al. [33] with modifications consistent with unpublished research of V. Axer. This leads to the following manufacturing process: 5 g of gelatine is slowly dissolved in 15 mL of distilled water at 55°C under continuous stirring. As all gelatine is dissolved, 2 g of glycerol and 2 mL of ethanol are added. After 2 min of stirring, 77.4 µL of a 37 %-formaldehyde solution is added, and the mixture is stirred for another minute. Afterward, the solution is poured into the mold and stored in a fume hood overnight.

2.3 | Surface Analysis

Surface structure analysis is carried out using LM and CLM. All skin substitutes are measured at three distinct surface regions by both methods applying different magnifications. The magnifications used are 10×, 20×, 50×, and 100× for the CLM and 80×, 200×, and 500× for the LM. Concerning the LM, all data is generated from 2×2 stitching and stacking with 200 images. For CLM measurements, stitching is only applied for 10× magnification with 4×4 images.

In order to compare surface waviness and roughness, average surface roughness (R_a) and maximal surface roughness (R_z) are determined using CLM and LM. The waviness describes the macroscopic and the roughness of the microscopic surface irregularities. For LM, those parameters are determined at 80× and 200× magnification for each measuring site by evaluating three equidistant horizontal and vertical lines for a total of six distinct lines per measurement. For CLM, they are determined with horizontal and vertical lines at each pixel at each magnification. Concerning both methods, median correction for surface inclination was carried out. Differentiation between surface waviness and surface roughness is achieved by using different orders of magnification.

Waviness/roughness values obtained from the LM measurements at 80× and 200× magnification are summarized each as mean values after testing normal distribution (span test according to David; $p = 99\%$) and eliminating outliers (Grubbs-test; $p = 99\%$). These mean values and a reference given by literature [43–45] are tested for variance homogeneity (F-test; $p = 99\%$) and compared using a T-test ($p = 99\%$). If no variance homogeneity is given, the comparison is carried out by the difference in standard deviations from the measured mean and the references median and whether the measured mean within its standard deviation overlaps the interquartile range (IQR) of the reference. However, the waviness/roughness values from the CLM are not tested for normal distribution and outliers due to sample sizes exceeding the range of statistical tests. Nevertheless, the data is summarized as mean values because normal distribution is expected for a random sample of sufficient sample size. The subsequent comparison is carried out using the IQR method described above.

2.4 | IR Spectroscopy and pH

ATR-Fourier Transformation Infrared (FTIR) spectra of all skin substitute materials are recorded. For each a mean spectrum from threefold measurement is calculated. VitroSkin, a hygroscopic material, is dried in a desiccator overnight. The spectra are recorded from 4000 to 500 cm^{-1} with 4 cm^{-1} bandwidth and 64 scans.

Additionally, the surface pH of skin substitutes is measured using a Skin-pH-Meter. The measurements are conducted threefold at three distinct regions.

2.5 | Mechanical Properties

Elastic properties of skin substitutes, especially viscoelastic ratio, relative elastic recovery, and relative remaining skin deformity,

are determined using a Cutometer. The analyzed parameter is the penetration depth of the skin substitute inside the probe, measured threefold at three different surface regions. For skin penetration measurements, a negative pressure of 450 mbar is applied for 3 s with continuing penetration depth measurement for 3 s after pressure release. For reproducible results, molded substitutes with a layer thickness of 1 mm were used. To achieve such a defined thickness, a dedicated mold was built in-house.

Another mechanical property measured is the friction of the skin substitute using a Frictionometer. The probe loads a circular Teflon surface of 2 cm diameter with 0.7 N and measures the friction in arbitrary units (AU) while spinning the Teflon surface at 225 rpm for 30 s. This parameter is measured twice at three distinct surface regions.

3 | Results

3.1 | Surface Structure and Waviness/Roughness Analysis

As all human beings are individuals, so is the detailed skin structure. The structure additionally depends on the specific age and body part. Nonetheless, it is possible to identify a common structure modulating the contact area between a TTS and the human skin.

It is not, to our knowledge, as of yet known to which extend the surface structure and its micro-texture influence adhesion to skin. Hence, both need to be evaluated. Therefore, 80× magnification LM and 10× magnification CLM images are utilized to characterize the macroscopic surface structure, while 500× magnification LM images, as well as 20×, 50×, and 100× magnification CLM images, are applied correspondingly to identify the micro-texture. A selection of microscopic images is presented in Figure 1.

As additional, quantitative parameters, the surface waviness and roughness are chosen. Metaphorically speaking, the dunes in a desert describe the desert's waviness, whereas the single grains of sand resemble the deserts roughness. To differentiate waviness and roughness, different magnifications are applied. Even though the relevance of waviness/roughness for adhesion to the skin has not been researched yet, the literature states that other adhesion processes depend on these characteristics [46, 47]. All results from the surface waviness and roughness analysis are depicted in Figures 2 and 3.

In accordance with those figures, molded skin substitute materials, especially Dragon Skin and modified gelatine, mimic the topography of human skin best. Deficiencies in roughness and waviness are only clearly observable for Gelafix and PU. However, from a structural point of view, Gelafix and VitroSkin show insufficient similarity to human skin.

3.2 | Surface Functionality

Despite the distinct importance of skin-like topography, the surface's functionality should not be neglected. As molecular and

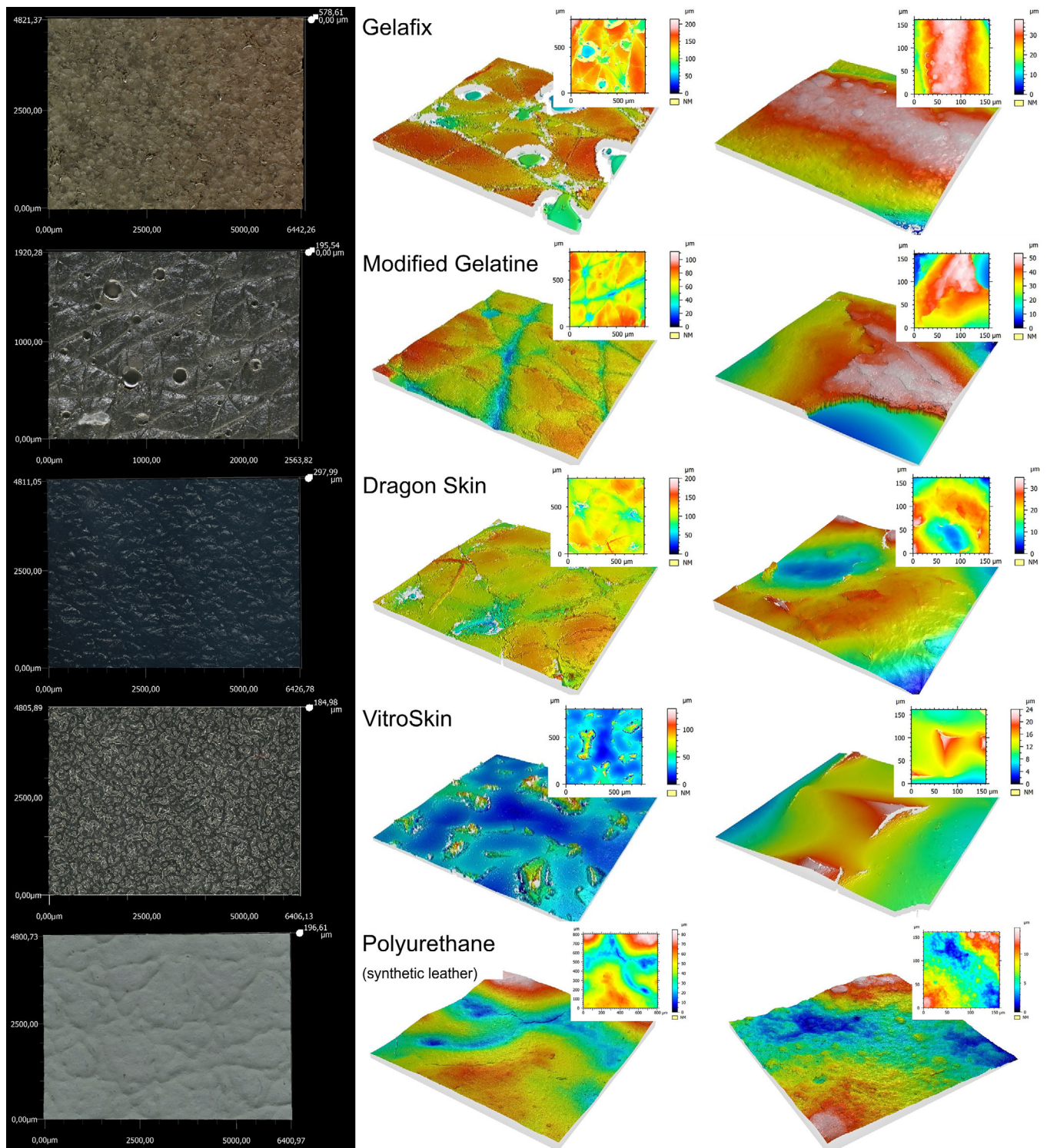


FIGURE 1 | Microscopic analysis of skin substitutes surface structure using (left) 80× magnification with 2 × 2 stitching LM (4.8 × 6.4 mm), (middle) 20× magnification CM (0.8 × 0.8 mm) and (right) 100× magnification CM images (0.15 × 0.15 mm). From top to bottom, the skin substitute materials are Gelafix, modified gelatine, Dragon Skin, VitroSkin, and synthetic leather based on polyurethane.

thermodynamic interactions between two adhering surfaces are important in general [47–52], it is assumed to be of significance for adhesion to skin as well.

An effective approach to evaluate the functionality of skin substitute materials is the application of IR spectroscopy. It has been commonly applied to investigate skin surface functional

groups in literature for normal and defatted human skin [53–55]. The skins most important functional groups are carbonyl groups (C = O), secondary amine groups (N–H), ester groups (COO), hydroxy groups (OH), primary amine groups (H–N–H) and carboxylic acid groups (COOH) [56]. Table 1 shows which of these functional groups are found in the skin substitute materials tested. Additionally, for dedicated interpretation all mean spectra

TABLE 1 | Evaluation of skin similarity of skin substitutes regarding surfaces functional groups.

Materials	Functional groups					
	COOH	NH ₂	OH	COO	NH	CO
PU	—	—	—	+	+	+
Dragon Skin	—	—	—	—	—	—
Dragon Skin (Silflo)	—	—	+	—	—	—
Gelatine	+	+	+	+	+	+
Gelafix	+	+	+	+	+	+
VitroSkin	+	+	+	+	+	+

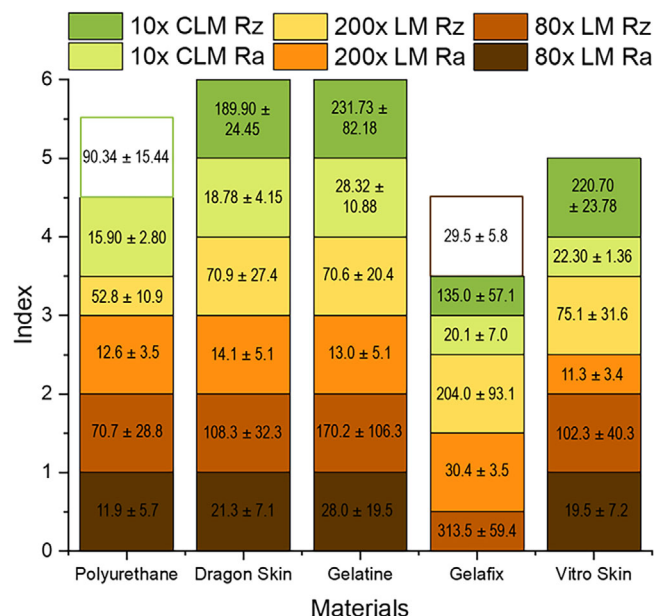


FIGURE 2 | Evaluation of skin similarity of skin substitutes regarding surfaces waviness. Inside each box, the parameters’ measured values are given with mean and standard deviation in μm. All uncolored, but framed boxes display the surface waviness values that are not congruent with the given reference (similarity index of 0). Therefore, only colored boxes represent skin similarity. The displayed parameters are the average surface roughness (R_a) and the maximal surface roughness (R_z) measured using a confocal light microscope (CLM) or a light microscope (LM) at 10×, 80×, or 200× magnification.

of the presented materials and a reference spectrum are presented in Figure 4.

Out of these materials, VitroSkin, Gelafix, and modified gelatine show all characteristic bands of human skin, and no bands of functional groups not associated with human skin. Functionality-wise, the other materials are significantly different from human skin.

3.3 | Skin Probes

A convenient and widely used approach to determine skin characteristics in dermatology and cosmetics are skin probe systems. In this case, such probes are used to determine the pH,

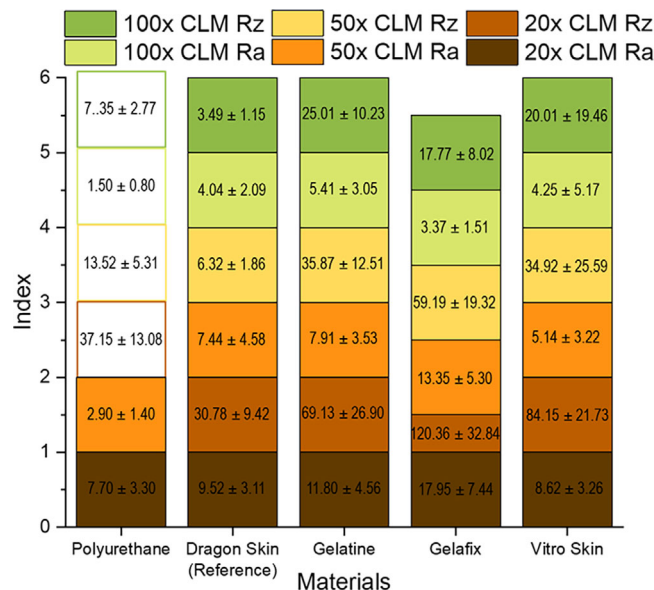


FIGURE 3 | Evaluation of skin similarity of skin substitutes regarding surfaces roughness. Inside each box, the parameters’ measured values are given with mean and standard deviation in μm. All uncolored, but framed boxes display the surface roughness values that are not congruent with the given reference (similarity index of 0). Therefore, only colored boxes represent skin similarity. The displayed parameters are the average surface roughness (R_a) and the maximal surface roughness (R_z) measured using a confocal light microscope (CLM) at 20×, 50×, or 100× magnification.

friction, and elasticity of skin substitutes. All results are depicted in Figures 5 and 6 with the respective standard deviations. The results will be evaluated in detail in the following chapter.

4 | Discussion

4.1 | Surface Structure and Roughness Analysis

To compare the portrayed results for the skin substitutes with actual human skin surface structure, references are provided by the works of Dabrowska et al. [43], Derler et al. [45], and Lagarde et al. [57]. However, no robust reference can be found in the literature regarding high-magnification images for the microtextural characterization to the best of the author’s knowledge. Despite this, a reference is essential for comparison of human skin with

TABLE 2 | Reference values for the analysis of skin substitutes surface roughness from casted Dragon Skin.

Magnification	Mean (R_a) in μm	Median (R_a) in μm	IQR (R_a) in μm	Mean (R_z) in μm	Median (R_z) in μm	IQR (R_z) in μm
20× CM	9.52 ± 3.1	9.20	7.1–11.2	81.69 ± 17.70	81.1	70.2–82.8
50× CM	7.44 ± 4.58	5.96	4.2–9.6	42.33 ± 18.46	37.59	28.3–54.9
100× CM	4.04 ± 2.09	3.50	2.7–5.0	7.35 ± 2.77	22.52	13.0–27.2

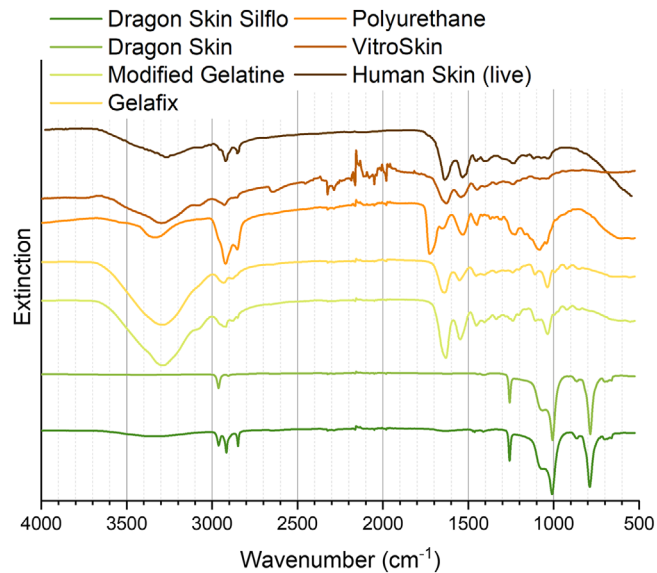


FIGURE 4 | Mean spectra of ATR-FTIR analysis of skin substitute materials compared to Human Skin (live) from Thermo Scientific Common Materials database.

the tested materials. As the use of polydimethylsiloxane (PDMS) skin replicas for microscopic purposes is common practice in the scientific literature [33, 43–45, 57], a skin replica from Dragon Skin is used as a reference (Table 2).

Regarding the observed surface structures and micro textures, VitroSkin deviates the most from real skin. It is dominated by sharp edges on a smooth surface, yet some parallels can be observed. Only distantly, the protrusions from the sharp edges resemble a skin-like pattern.

A better approximation is synthetic leather, as the surface structure mimics the skin relief of mammalian leather. Nevertheless, the relief is widely meshed with soft edges and, therefore, deviates from human skin. The deviations from human skin increase as the microstructure is taken into account, as it does not approximate human skin at all. As synthetic leather is only meant to mimic the appearance of real leather, microstructures are not taken into consideration during manufacturing.

Those considerations are made for materials cast using a skin imprint. Hence, their surface structures are closest to human skin. Still, significant differences in surface quality are observed due to differing material properties leading to different quality replicas. The most challenging approaches are those that utilize modified gelatine, especially Gelafix. Due to its significant viscosity, air is trapped during preparation. As the air cannot escape due

to the rapid hardening, the result is a heavily impaired surface structure. Not regarding the affected surface area, the material resembles both the surface structure and micro texture of human skin. Therefore, reducing the affected area by decreasing the amount of entrapped air is highly advantageous. One possibility is heating granulated Gelafix inside a heat-resistant mold. As no transfer is needed, the amount of entrapped air would be minimized. However, sample preparation inside the mold is impossible for modified gelatine due to its various preparation steps. Alternatively, degassing the heated gelatine solution in vacuo can reduce the entrapped air. As the issue of entrapped air does not occur using Dragon Skin, it replicates the surface structure and micro texture of human skin satisfactorily.

In addition to the qualitative parameters of surface structure and micro texture, quantitative parameters such as waviness and roughness are needed for a holistic characterization and comparison. Such comparison requires references from the scientific literature. As the sample size from each publication alone is insufficient to represent the population, results from different studies related to different body sites are comprehended as weighted means ($R_a = 18.9 \mu\text{m}$; $R_z = 82.3 \mu\text{m}$) with weighted standard deviations ($R_a = 4.7 \mu\text{m}$; $R_z = 21.2 \mu\text{m}$) weighted by corresponding sample sizes and as median ($R_a = 18.0 \mu\text{m}$; $R_z = 78.4$) with IQR (R_a : 16.2–20.1 μm ; R_z : 71.6–83.3), respectively [43–45]. The resulting sample size of 139 approximates the population better and gives weight to the presented compendium. As those references arise primarily from profilometer measurements, they resemble only the macroscopic surface waviness. Due to the lack of references regarding microscopic surface roughness in literature, casted Dragon Skin is used as a reference (Table 2).

The similarity between a substitute’s waviness/roughness and human skin is depicted in Figures 2 and 3, respectively. The similarities are described by the index of each roughness/waviness parameter. An index value of 1 denotes that no statistical differentiation between reference and skin substitute is possible. The index value is reduced to 0.5 if no *t*-test is possible due to variance inhomogeneity and only one of two alternative similarity criteria (± 1 standard deviation around the tested mean within the references IQR; references median within ± 2.58 standard deviations around the tested mean) is fulfilled. Only if a *t*-test allows the differentiation or no alternative similarity criteria is fulfilled, the index value is reduced to 0. All parameters’ indices are summed up for overall comparability of waviness/roughness, leading to an overall index between 0 and 6.

According to the indexing system, synthetic leather’s and Gelafix’s waviness deviate the most from human skin. The remaining substitutes resemble the surface waviness of human

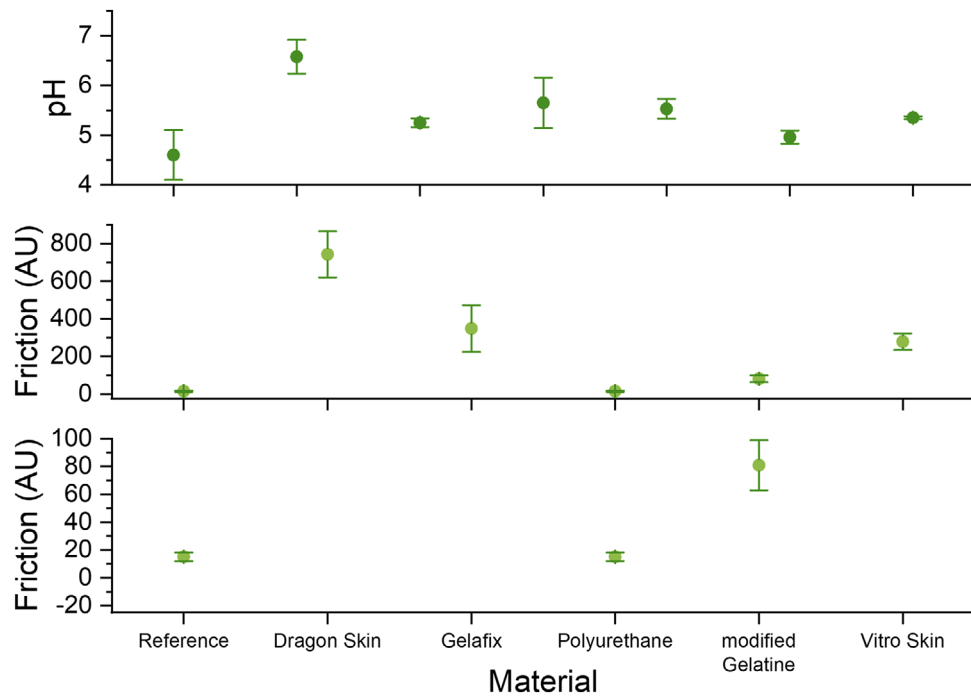


FIGURE 5 | Skin similarity evaluation of different skin substitute materials regarding (top) their surface pH measured using a Skin-pH-Meter and (middle & bottom) their frictional properties measured with a Frictiometer.

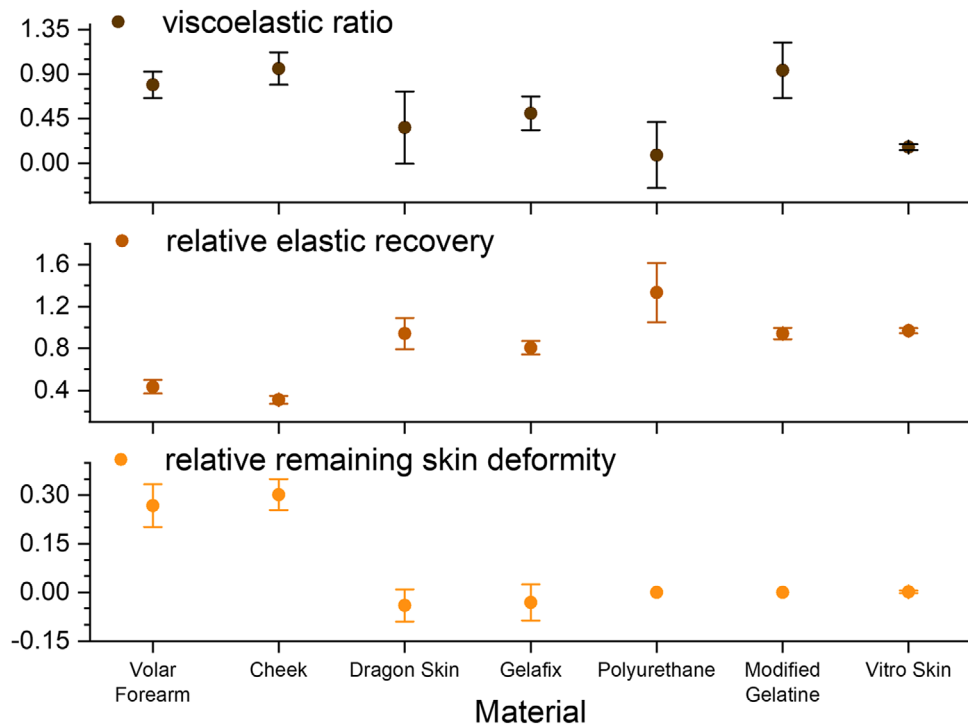


FIGURE 6 | Skin similarity evaluation of different skin substitute materials regarding their elasticity measured using a Cutometer. The materials are compared to a human reference regarding their (top) viscoelastic ratio, (middle) relative remaining skin deformity, and (bottom) relative elastic recovery.

skin, and comparable results are achieved concerning the surface roughness. Despite Gelafix's strong deviations from human skin waviness, its roughness is mostly comparable to human skin. As only small surface areas can be analyzed regarding the surface's roughness, the impaired areas of Gelafix's surface are

not statistically comparable considered. Synthetic leather only mimics human skin for R_a at lower magnifications. In contrast to R_a , R_z is calculated from the distances between the highest ridges and deepest rifts. Therefore, R_z is sensitive for surface inhomogeneities. This sensitivity can easily lead to significant

differences between nearly similar surfaces. However, all other skin substitutes are indistinguishable from human skin.

4.2 | Surface Functionality

For a detailed evaluation of the skin substitutes' surface functionality, not only the most important functional groups need to be considered, but the whole spectra too. For comparison with human skin, a reference spectrum of live human skin from the Thermo Scientific Common Materials database is used.

Out of all the tested materials, only VitroSkin, Gelafix, and modified gelatine show characteristic bands of only all the relevant functional groups associated with human skin (Table 1 & Figure 4).

The best of those three skin substitutes regarding IR-activity is VitroSkin, as its spectrum is nearly congruent to human skin if issues due to water absorption and CO₂ are neglected. The only significant difference is a considerably weaker NH bending vibration at 652 cm⁻¹. Other main vibrations are a C = O overtone at 3760 cm⁻¹, an amide and amine NH stretch between 3500 and 3120 cm⁻¹, an acidic OH stretch at 3290 cm⁻¹, an alkene CH stretch at 3084 cm⁻¹, an amide NH bending and C = O stretching at 1628 cm⁻¹ and a ring breath at 1450 cm⁻¹.

Nevertheless, regarding its IR spectrum, human skin and Gelafix are nearly identical, too. The only major difference is that gelatine, in general, does not show a ring breath vibration and, therefore, no aromatic ring structure. Additionally, other occurring variations are a weaker NH bending vibration at 650 cm⁻¹ and a strongly increased acidic OH stretching at 3289 cm⁻¹ due to extensive amounts of glycerol as a plasticizing agent. However, amide and amine NH stretches between 3550 and 3100 cm⁻¹, an alkene CH stretching at 3060 cm⁻¹, and an amide NH bending overlapped by C = O stretching at 1640 cm⁻¹ correspond to human skin with minor deviations. The same holds true for modified gelatine.

Polyurethane (Table 1) shows lower similarity to human skin regarding its functionality. An NH stretching vibration band is seen at 3336 cm⁻¹ with its corresponding bending vibration band at 600 cm⁻¹. The CN bending, on the other hand, overlaps with the C = O stretching of polyurethane at 1727 cm⁻¹. No band associated with carboxylic acids can be found. However, the necessity of these functional groups may be negligible as C = O is still present, and NH is comparable to OH in that both groups consist of a hydrogen atom being bonded to a strongly electronegative atom with at least one lone pair. Overall, compared to normal human skin, the bands of polyurethane are shifted towards higher wavenumbers (Figure 4). This shift is associated with shorter excitation wavelengths and, therefore, presumably stronger bonds in polyurethane. In contrast to polyurethane, human skin consists, among other, of collagen, existing in a helical structure [58, 59]. As helical structures are caused by intramolecular interactions, an intramolecular cause regarding the excitation wavelength is assumed. One prominent intramolecular interaction is hydrogen bonding. The added mass of hydrogen lowers the vibration frequency of the respective bond and decreases the corresponding wavenumber.

The highest deviation from human skin can be observed for Dragon Skin. Except for CH₃ symmetric and asymmetric stretching at 2963 and 2905 cm⁻¹, no similarities are present. Regarding this material, characteristic bands of SiCH₃ symmetric and asymmetric bending at 1412 and 1258 cm⁻¹ can be found. Additionally, a SiCH₃ stretching vibration at 785 cm⁻¹ and a characteristic SiOSi vibration at 1007 cm⁻¹ can be seen [60]. This corresponds to PDMS [61, 62]. Despite the differing functionality, the similarities of carbon and silicon are not to be neglected. Therefore, SiOSi groups may imitate carbon and oxygen bonding in real human skin. Additionally, an alcoholic OH stretching vibrations appears at 3350 cm⁻¹ as the catalyzer from the mold migrates into the casted Dragon Skin [60].

4.3 | Skin Probes

To evaluate the results from this dermatological approach to skin characterization, references of real human skin are inevitable. Fortunately, such references are given in scientific literature. For skin pH, given values [63–67] are summarized as weighted mean with its respective weighted standard deviation to enlarge the tested population. This summarization leads to a reference pH of 4.6 ± 0.5 with a sample size of 79. However, all substitute materials but VitroSkin do not contain artificial skin lipids. As skin lipids are acidic, they lower the surface pH. Therefore, these measurements serve only as a baseline. The materials are only accepted as skin-like if the surface pH is above the reference range, as the reference range is described by the pH of normal human skin with its naturally occurring lipid film. This is based on the assumption that the surface pH is significantly reduced by artificial skin lipids, and thus, a substitute in the reference range would, therefore, no longer be in it.

According to the results illustrated in Figure 5, all substitutes but modified gelatine are above the reference range for normal, lipid containing human skin. Therefore, modified gelatine and VitroSkin—the only material already containing lipids—seem unsuitable for the simulation of human skin in this regard. As artificial skin lipids will be added in further studies, these results are prone to change, and no final conclusions will be drawn.

Regarding skin friction, the biggest and most representative study was carried out among the Asian population. Therefore, the applicability for Caucasians or Africans may be limited. Despite this limitation, the data is used as a reference due to limited research. Overall, the reference is given as a weighted mean with a weighted standard deviation of 15 ± 3 AU with a sample size of 481 [68]. Out of all tested materials, only polyurethane is indistinguishable from human skin. However, it is expected that artificial skin lipids will act as lubricants and will decrease the friction between the surface and the probe. Therefore, these results serve as a baseline as well.

Lastly, skin probes are used to evaluate the elastic properties of substitute materials. In the literature, skin's viscoelastic ratio, relative elastic recovery, and remaining skin deformity are described [69]. As a reference for these characteristics, 95% confidence intervals reported for the volar forearm and the cheek are applied. According to Figure 6, only Dragon Skin and Gelafix resemble the viscoelastic ratio of human skin as the only properly

TABLE 3 | Weighting factors of the Skin Similarity Index.

Category	Factor
Surface structure	1
Micro texture	1
Waviness	2
Roughness	2
Functional groups	3
pH value	1
Elasticity	2
Friction	0.5

resembled characteristic. However, only relative characteristics are presented, and the absolute penetration depth of a substitute’s surface into the skin probe is not considered. This consideration is of further interest. Nevertheless, only relative characteristics are described in the literature to the best of the author’s knowledge, and new studies are needed for the evaluation of absolute penetration.

4.4 | Skin Similarity Index

As a great number of parameters are evaluated, an overview for the substitutes similarity to human skin is required. However, no data fusion system for skin similarities is described in literature yet to the best of the authors’ knowledge. Therefore, a mid-level data fusion system needs to be established to build the foundation for holistic evaluation of a skin substitutes similarity to human skin.

For this purpose, the data is divided into eight different categories: Surface structure, micro texture, waviness, roughness, surface functional groups, pH-value, friction, and elasticity. Each is described by an index between zero and one whereas zero indicates no similarity to human skin and is undifferentiable. This approach equals the system used for surface roughness and waviness evaluation and is used for all parameters of each category. To convert all parameters of a category to a category’s index value, the summed-up indices of the parameters are divided by the number of parameters. To sharpen the profile of the indexing system, the eight categories are weighted according to Table 3. The weighting results from generally know dependency of adhesion but is not based on knowledge of adhesion to skin. Therefore, this is only a hypothesized weighting, and further research is necessary to develop a final weighting system.

However, it is to be expected that surface roughness and waviness have a significant impact on the adhesion to the skin as these categories showed a distinctive correlation to adhesion in previous studies [46, 70]. Therefore, both are double-weighted. The same holds true for elasticity. As an elastic surface creates more stress to the TTS due to enhanced tension and compression, and generates a changing angle during the peel-off of a TTS, it is expected to influence the adhesion to skin significantly. Another particularly interesting category are the functional groups. Previous studies have established a relation between molecular interactions and

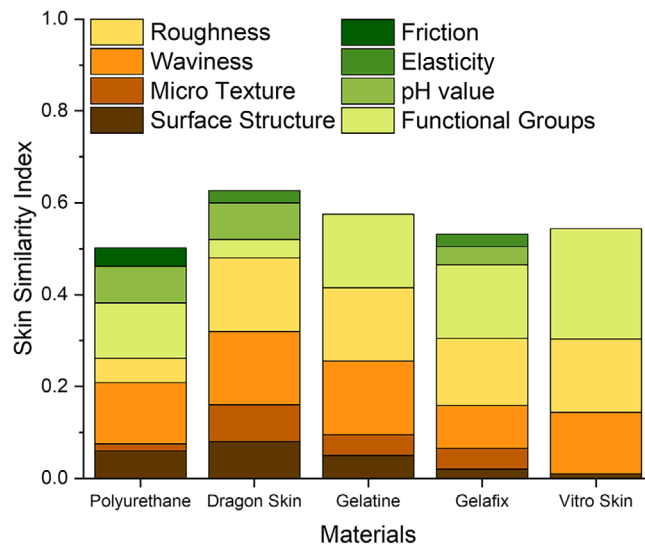


FIGURE 7 | Skin similarity evaluation of skin substitutes over all analyzed categories. The maximal achievable index value is 1.

adhesion, linking the molecular interactions to the functional groups of the surface [49, 70, 48]. Therefore, this category is given the triple weight. As the pH value of a surface is strongly dependent on the chemical functionality of a surface, it is weighted with a factor of 1. This leads to a balance between the weighting of surface roughness/waviness and the chemical functionality, which are strongly expected to influence the adhesion to skin significantly. The last modified weighting factor is for friction. Due to the process of adhesion, only minor relevance for the adhesion to the skin is expected, and therefore, it is weighted with a factor of 0.5.

In order to present the results in a clear and comprehensible manner, the indices of the individual categories are standardized by the sum of the weighting factors. This results in a Skin Similarity Index between 0 (no similarity to skin) and 1 (indistinguishable from skin [Figure 7]).

According to Figure 7, the best substitutes are modified Gelatine and Dragon Skin. Their individual strengths and weaknesses are shown in Table 4. Despite Dragons Skins strength regarding its topography, it lacks the functional groups of human skin as well as its frictional properties and its elasticity. Considering these properties, polyurethane seems more suited as a skin substitute material. However, it scores the lowest Skin Similarity Index and is, therefore, the less suitable substitute material.

4.5 | Limitations

As stated in the introduction, this study’s aim is to lay the foundation for further research. As the foundational study and, therefore, fundamental research, a broad baseline for future studies is established. However, as fundamental research suggests, the presented models and methods still have significant limitations. Most strikingly, the analyzed materials and characteristics are based on literature regarding adhesion in general and experience from the industry, whereas the concepts are applicable to all usages of skin substitutes. However, this research is specifically

TABLE 4 | Qualitative strengths (+) and weaknesses (–) of skin substitute materials compared to each other. The mechanical behavior combines the categories “Elasticity” and “Friction” of the Skin Similarity Index. Accordingly, “Surface Functionality” includes the pH value and the surface functionalities, and “Topography” contains the features of waviness, roughness, surface structure, and micro texture.

Skin substitute material	Mechanical behavior	Surface functionality	Topography
Polyurethane	+	0	0
Dragon Skin	+	—	+
Gelatine	—	0	+
Gelafix	+	+	0
VitroSkin	—	+	—

designed to match the requirements of in vitro adhesion testing. As adhesion is a superficial process, the presented data or, more precisely, the use of the presented data is limited to in vitro superficial processes only. Even though these limitations exclude permeation testing or application in emergency medicine, it may be used for developing in vitro test systems for distribution or deposition on skin. However, for this data to be used in those fields of application, different “Skin Similarities Indices” are needed. The indexing system is customized for each application by different weighting factors. Therefore, the conclusion from the indexing system are individual for each application. However, without further research, the weighting factors are only estimates based on scientific literature. Hence, no final conclusions can be made whatsoever, and only, still most importantly, is the foundation for dedicated further research regarding different practical, user-oriented topics on product performance tests on human skin is provided.

5 | Conclusion

In summary, a system to rate similarity to human skin incorporating topography, mechanical characteristics, and chemical functionality is established. This system is applied to a broad range of skin substitute materials for adhesion testing of TTS and leads to Dragon Skin and modified gelatine as best-suited materials. However, PU seems to be a more rounded material as it scores in most aspects, is inexpensive, and does not need any preparation to be used.

Anyway, most tested materials lack artificial skin lipids that need to be added in further research. Such coatings are widely described in the literature [28, 49, 50, 71–74]. This modification of materials would not only lead to more accurate results for friction, pH, and surface functionality but would also allow a first discrimination between different skin types (oligoseborrheic, nomoseborrheic, and hyperseborrheic).

Furthermore, artificial skin lipids would change the surfaces’ contact angle too. Contact angle analysis under the application of the Van-Oss-model [75] is commonly used to characterize human skin [53, 76–79]. As it describes the hydrophilia and lipophilia of a surface, it is suspected to have a significant effect on adhesive properties.

Additionally, the reproducibility of the substitute itself must be taken into consideration, as only a reproducible skin substitute

can lead to reproducible adhesion testing. However, all materials that need to be casted possess an inherent lack of reproducibility. As each mold is unique, no standard can be applied yet, and all results are dependent on the individual skin imprint. This issue needs to be solved for future industrial applications.

After all, the most important task in developing a skin substitute for adhesion simulation of TTS is the correlation of adhesion tests using different skin substituent materials with data from real human skin. This is inevitable in evaluating the relevance of all characteristics and engineering an applicable skin substitute. The presented study lays the foundation for consistent, in-depth research in this field.

Acknowledgments

The authors thank the German Federal Ministry of Education and Research (BMBF) for funding the research project “Optimization of the adhesion behavior of transdermal therapeutic systems on soft substrates and their simulation” (grant number 13FH022KX1). Additionally, the authors would like to thank Courage + Khazaka GmbH for providing the different used skin probe systems used in this study.

Open access funding enabled and organized by Projekt DEAL.

Ethics Statement

The authors confirm that the ethical policies of the journal, as noted on the journal’s author guidelines page, have been adhered to.

Conflicts of Interest

The authors declare no conflicts of interest.

Data Availability Statement

The data that support the findings of this study are available from the corresponding author upon reasonable request.

References

1. M. Sheikholeslam, M. Wright, M. Jeschke, et al., “Biomaterials for Skin Substitutes,” *Advanced Healthcare Materials* 7 (2018): 1700897.
2. R. O. Potts and M. L. Francoeur, “Lipid Biophysics of Water Loss Through the Skin,” *Proceedings of the National Academy of Sciences of the United States of America* 87 (1990): 3871–3873.
3. A. A. Romanovsky, “Skin Temperature: Its Role in Thermoregulation,” *Acta Physiologica* 210 (2014): 498–507.

4. S. Venkatraman and R. Gale, "Skin Adhesives and Skin Adhesion 1. Transdermal Drug Delivery Systems," *Biomaterials* 19 (1998): 1119–1136.
5. P. Minghetti, F. Cilurzo, and A. Casiraghi, "Measuring Adhesive Performance in Transdermal Delivery Systems," *Technology Tools* 2 (2004): 193–206.
6. DIN ISO 29562:2018 (2018), Self Adhesive Tapes Determination of Peel Adhesion Properties. (ISO 29652:2018).
7. DIN ISO 29863:2018 (2018), Self Adhesive Tapes Measurement of Static Shear Adhesion. (ISO 29863:2018).
8. I. Jones, L. Curie, and R. Martin, "A Guide to Biological Skin Substitutes," *British Journal of Plastic Surgery* 55 (2002): 185–193.
9. J. Jean, M. E. Garcia-Pérez, and R. Pouliot, "Bioengineered Skin: The Self-Assembly Approach," *Journal of Tissue Science and Engineering S* (2011): 05.
10. T. T. Nyame, H. A. Chiang, and D. P. Orgill, "Clinical Applications of Skin Substitutes," *Surgical Clinics of North America* 94 (2014): 839–850.
11. S. T. Boyce, "Cultured Skin Substitutes: A Review," *Tissue Engineering* 2 (1996): 255–266.
12. J. C. Geesin, L. Brown, Z. Liu, et al., "Development of a Skin Model Based on Insoluble Fibrillar Collagen," *Journal of Biomedical Materials Research Part B: Applied* 33 (1996): 1–8.
13. C. Castagnoli, M. Fumagalli, D. Alotto, et al., "Preparation and Characterization of a Novel Skin Substitute," *Journal of Biomedicine and Biotechnology* 2010 (2010): 840363.
14. L. Alrubaiy and K. K. Al-Rubaiy, "Skin Substitutes: A Brief Review of Types and Clinical Applications," *Oman Medical Journal* 24 (2009): 4–6.
15. J. T. Shores, A. Gabriel, and S. Gupta, "Skin Substitutes and Alternatives: A Review," *Advances in Skin & Wound Care* 20 (2007): 509–511.
16. S. Böttcher-Haberzeth, T. Biedermann, and E. Reichmann, "Tissue Engineering of Skin," *Burns* 36 (2010): 450–460.
17. T. T. Nyame, H. Chiang, T. Leavitt, et al., "Tissue – Engineered Skin Substitutes," *Plastic and Reconstructive Surgery* 136 (2015): 1379–1388.
18. M. Leroy, M. Lafleur, M. Auger, et al., "Characterization of the Structure of Human Skin Substitutes by Infrared Microscopy," *Analytical and Bioanalytical Chemistry* 405 (2013): 8709–8718.
19. D. Kocsis, H. Kichou, K. Döme, et al., "Structural and Functional Analysis of Excised Skins and Human Reconstructed Epidermis with Confocal Raman Spectroscopy and in Microfluidic Diffusion Chambers," *Pharmacy* 14 (2022): 1689.
20. G. E. Flaten, Z. Palac, A. Engesland, et al., "In Vitro Skin Models as a Tool in Optimization of Drug Formulation," *European Journal of Pharmaceutical Sciences* 75 (2015): 10–24.
21. N. E. Biondo, D. F. Argenta, and T. Caon, "A Comparative Analysis of Biological and Synthetic Skin Models for Drug Transport Studies," *Pharmaceutical Research* 40 (2023): 1209–1221.
22. R. Neupane, S. Boddu, J. Renukuntla, et al., "Alternatives to Biological Skin in Permeation Studies: Current Trends and Possibilities," *Pharmacy* 12 (2020): 152.
23. L. Hagvall, M. Munem, M. Hoang Philipsen, et al., "Skin Permeation Studies of Chromium Species—Evaluation of a Reconstructed Human Epidermis Model," *Toxicology in Vitro* 91 (2023): 105636.
24. K. Ghosal, S. Thomas, N. Kalarikkal, et al., "Collagen Coated Electrospun Polycaprolactone (PCL) with Titanium Dioxide (TiO₂) from an Environmentally Benign Solvent: Preliminary Physico-Chemical Studies for Skin Substitute," *Journal of Polymer Research* 21 (2014): 410.
25. K. Ghosal, A. Manakhov, L. Zajíčková, et al., "Structural and Surface Compatibility Study of Modified Electrospun Poly(ϵ -Caprolactone) (PCL) Composites for Skin Tissue Engineering," *Aaps Pharmscitech [Electronic Resource]* 18 (2017): 72–81.
26. Florida Suncare Testing, Inc. (Publisher), VITRO-SKIN The Global Standard for Rapid, Predictive In Vitro Testing. Accessed November 14 2023, <https://ims-usa.com/vitro-skin-substrates/vitro-skin/>.
27. S. Chen and B. Bhushan, "Nanomechanical and Nanotribological Characterization of Two Synthetic Skins with and Without Skin Cream Treatment Using Atomic Force Microscopy," *Journal of Colloid & Interface Science* 398 (2013): 247–254.
28. F. Eudier, M. Grisel, G. Savary, et al., "Design of a Lipid-Coated Polymeric Material Mimic Human Skin Surface Properties: A Performing Tool to Evaluate Skin Interaction with Topical Products," *Langmuir* 36 (2020): 4582–4591.
29. Kryolan GmbH (Publisher), Gelafix Haut. Accessed November 14 2023, <https://de.kryolan.com/produkt/gelafix-haut#yellow>.
30. F. Fayyazbakhsh and M. C. Leu, "A Brief Review on 3D Bioprinted Skin Substitutes," *Procedia Manufacturing* 48 (2020): 790–796.
31. P. Sobhanian, M. Khorram, S. Hashemi, et al., "Development of Nanofibrous Collagen-Grafted Poly (Vinyl Alcohol)/Gelatin/Alginate Scaffolds as Potential Skin Substitute," *International Journal of Biological Macromolecules* 130 (2019): 977–987.
32. F. Eudier, G. Savary, M. Grisel, et al., "Skin Surface Physico-Chemistry: Characteristics, Methods of Measurement, Influencing Factors and Future Developments," *Advances in Colloid and Interface Science* 264 (2019): 11–27.
33. I. Lir, M. Haber, and H. Dodiuk-Kenig, "Skin Surface Model Material as a Substrate for Adhesion-to-Skin Testing," *Journal of Adhesion Science and Technology* 21 (2007): 1497–1512.
34. J.-E. Lee, J. C. Park, Y. S. Hwang, et al., "Characterization of UV-Irradiated Dense/Porous Collagen Membranes: Morphology, Enzymatic Degradation, and Mechanical Properties," *Yonsei Medical Journal* 42 (2001): 172–179.
35. L. H. H. Olde Damink, P. Dijkstra, M. Van Luyn, et al., "Crosslinking of Dermal Sheep Collagen Using Hexamethylene Diisocyanate," *Journal of Materials Science: Materials in Medicine* 6 (1995): 429–434.
36. M. E. Nimni, D. Cheung, B. Strates, et al., "Chemically Modified Collagen: A Natural Biomaterial for Tissue Replacement," *Journal of Biomedical Materials Research* 21 (1987): 741–771.
37. K. S. Weadock, E. Miller, E. Keuffel, et al., "Effect of Physical Crosslinking Methods on Collagen-Fiber Durability in Proteolytic Solutions," *Journal of Biomedical Materials Research* 32 (1996): 221–226.
38. N. Davidenko, D. Bax, C. Schuster, et al., "Optimisation of UV Irradiation as a Binding Site Conserving Method for Crosslinking Collagen-Based Scaffolds," *Journal of Materials Science: Materials in Medicine* 27 (2016): 14.
39. G. Wollensak, E. Spoerl, and T. Seiler, "Riboflavin/Ultraviolet-a-Induced Collagen Crosslinking for the Treatment of Keratoconus," *American Journal of Ophthalmology* 223: 620–627.
40. Florida Suncare Testing, Inc. (Publisher), IMS In Vitro SPF/UVA Protocol for Use with VITRO-SKIN Substrate. Florida Suncare Testing, Inc. Bunnell no date.
41. MonaDerm. (Publisher), SILFLO: Silicone for Replica Making Process. MonaDerm Monaco no date.
42. Smooth-On, Inc. (Publisher), Dragon Skin TM Series Addition Cure Silicone Rubber Compounds. Smooth-On, Inc, Macungie no date.
43. A. K. Dabrowska, C. Adlhart, F. Spano, et al., "In Vivo Confirmation of Hydraton-Induced Changes in Human-Skin Thickness, Roughness and Interaction with the Environment," *Biointerphases* 11 (2016): 031015.
44. C. Edwards, R. Heggie, and R. Marks, "A Study of Differences in Surface Roughness Between Sun-Exposed and Unexposed Skin with Age," *Photodermatol Photoummunol Photomed* 19 (2003): 169–174.
45. S. Derler, L. Gerhardt, A. Lenz, et al., "Friction of Human Skin Against Smooth and Rough Glass as a Function of the Contact Pressure," *Tribology International* 42 (2009): 1565–1574.

46. M. Mu, S. Liu, W. DeFlorio, et al., "Influence of Surface Roughness, Nanostructure, and Wetting on Bacterial Adhesion," *Langmuir* 39 (2023): 5426–5439.
47. F. Awaja, M. Gilbert, G. Kelly, et al., "Adhesion of Polymers," *Progress in Polymer Science* 34 (2009): 948–968.
48. X. Ma, X. Zhou, J. Ding, et al., "Hydrogels for Underwater Adhesion: Adhesion Mechanism, Design Strategies and Applications," *Journal of Materials Chemistry A* 10 (2022): 11823–11853.
49. A. T. Salminen, K. J. Davis, R. P. Felton, et al., "Parallel Evaluation of Alternative Skin Barrier Models and Excised Human Skin for Dermal Absorption Studies In Vitro," *In Vitro Toxicology* 91 (2023): 105630.
50. K. Hori and S. Matsumoto, "Bacterial Adhesion: From Mechanism to Control," *Biochemical Engineering Journal* 48 (2010): 424–434.
51. X. Chen and T. Taguchi, "Enhanced Skin Adhesive Property of Hydrophobically Modified Poly(Vinyl Alcohol) Films," *ACS Omega* 5 (2020): 1519–1527.
52. E. Smit. (Lohmann GmbH), Friedland R. (Lohmann GmbH), Komenda M. LTS Lohmann Therapie-Systeme AG (personal conversation, 10.11.2023).
53. W. Youssef, R. R. Wickett, and S. B. Hoath, "Surface Free Energy Characterization of Vernix Caseosa. Potential Role in Waterproofing the Newborn Infant," *Skin Research and Technology* 7 (2001): 10–17.
54. C. Laugel, N. Yagoubi, and A. Baillet, "ATR-FTIR Spectroscopy: A Chemometric Approach for Studying the Lipid Organization of the Stratum Corneum," *Chemistry and Physics of Lipids* 135 (2005): 55–68.
55. R. O. Ports, D. Guzek, R. Harris, et al., "A Noninvasive, In Vivo Technique to Quantitatively Measure Water Concentration of the Stratum Corneum Using Attenuated Total-Reflectance Infrared Spectroscopy," *Archives of Dermatological Research* 277 (1985): 489–495.
56. J. Krawczyk, "Surface Free Energy of the Human Skin and Its Critical Surface Tension of Wetting in the Skin/Surfactant Aqueous Solution/Air System," *Skin Research and Technology* 21 (2015): 214–223.
57. J. M. Lagarde, C. Rouvrais, and D. Black, "Topography and Anisotropy of the Skin Surface with Ageing," *Skin Research and Technology* 11 (2005): 110–119.
58. B. B. Doyle, E. G. Bendit, and E. R. Blout, "Infrared Spectroscopy of Collagen and Collagen-Like Polypeptides," *Biopolymers* 14 (1975): 937–957.
59. B. de Campos Vidal and M. L. S. Mello, "Collagen Type I Amide I Band Infrared Spectroscopy," *Micron (Oxford, England: 1993)* 42 (2011): 283–289.
60. E. Pretsch, P. Bühlmann, and M. Badertscher, *Spektroskopische Daten zur Strukturaufklärung Organischer Verbindungen*, 5th ed. (Springer, 2010).
61. C. A. Canaria, I. Lees, A. Wun, et al., "Characterization of the Carbon-Silicon Stretch in Methylated Porous Silicon—Observation of an Anomalous Isotope Shift in the FTIR Spectrum," *Inorganic Chemistry Communications* 5 (2002): 560–564.
62. P. J. Launer and B. Arkles, *Silicon Compounds: Silanes & Silicones*, 3rd ed. (Gelest, 2013).
63. E. Berardesca, F. Pirot, M. Singh, et al., "Differences in Stratum Corneum pH Gradient When Comparing White Caucasian and Black African-American Skin," *British Journal of Dermatology* 139 (1998): 855–857.
64. A. Elkhyat, C. Courderot-Masuyer, S. Mac-Mary, et al., "Assessment of Spray Application of Saint GERVAIS Water Effects on Skin Wettability by Contact Angle Measurement Comparison with Bidistilled Water," *Skin Research and Technology* 10 (2004): 283–286.
65. R. Aly, C. Shirley, B. Cunico, et al., "Effect of Prolonged Occlusion on the Microbial Flora, pH, Carbon Dioxide and Transepidermal Water Loss of Human Skin," *Journal of Investigative Dermatology* 71 (1978): 378–381.
66. A. A. Hartmann, "Effect of Occlusion on Resident Flora, Skin-Moisture and Skin pH," *Archives of Dermatological Research* 275 (1983): 251–254.
67. H. Wagner, K. Kostka, C. Lehr, et al., "pH Profiles in Human Skin: Influence of Two In Vitro Test Systems for Drug Delivery Testing," *European Journal of Pharmaceutics and Biopharmaceutics* 55 (2003): 57–65.
68. Y. H. Zhu, S. Song, W. Luo, et al., "Characterization of Skin Friction Coefficient, and Relationship to Stratum Corneum Hydration in a Normal Chinese Population," *Skin Pharmacology and Physiology* 24 (2011): 81–86.
69. K. Selbmann, Querschnittsstudie zur Ermittlung von biomechanischen Hauteigenschaften mittels Cutometer und Reviscometer zur Ableitung von Richtwerten für gesunde Haut. Dissertation. 2012. University Medicine [print].
70. F. Awaja, M. Gilbert, G. Kelly, B. Fox, and P. J. Pigram, "Adhesion of Polymers," *Progress in Polymer Science* 34, no. 9 (2009): 948–968.
71. L.-C. Gerhardt, A. Schiller, B. Müller, et al., "Fabrication, Characterisation and Tribological Investigation of Artificial Skin Surface Lipid Films," *Tribology Letters* 34 (2009): 81–93.
72. A. B. Stefaniak, C. J. Harvey, and P. W. Wertz, "Formulation and Stability of a Novel Artificial Sebum Under Conditions of Storage and Use," *International Journal of Cosmetic Science* 32 (2010): 347–355.
73. A. B. Stefaniak and C. J. Harvey, "Dissolution of Materials in Artificial Skin Surface Film Liquids," *In Vitro Toxicology* 20 (2006): 1265–1283.
74. M. W. de Jager, G. Gooris, M. Ponc, et al., "Lipid Mixtures Prepared with Well-Defined Synthetic Ceramides Closely Mimic the Unique Stratum Corneum Lipid Phase Behavior," *Journal of Lipid Research* 46 (2005): 2649–2656.
75. S. Yang, L. Li, M. Lu, et al., "Determination of Solute Diffusion Properties in Artificial Sebum," *Journal of Pharmaceutical Sciences* 108 (2019): 3003–3010.
76. C. J. van Oss, R. J. Good, and M. K. Chaudhury, "Additive and Nonadditive Surface Tension Components and the Interpretation of Contact Angles," *Langmuir* 4 (1988): 884–891.
77. A. Mavon, D. Redoules, P. Humbert, et al., "Changes in Sebum Levels and Skin Surface Free Energy Components Following Skin Surface Washing," *Colloids and Surfaces B* 10 (1998): 243–250.
78. G. Percoco, A. Patatian, F. Eudier, et al., "Impact of Cigarette Smoke on Physical-Chemical and Molecular Properties of Human Skin in an Ex Vivo Model," *Experimental Dermatology* 30 (2021): 1610–1618.
79. A. Mavon, H. Zahouni, D. Redoules, et al., "Sebum and Stratum Corneum Lipids Increase Human Skin Surface Free Energy as Determined from Contact Angle Measurements: A Study on Two Anatomical Sites," *Colloids and Surfaces B* 8 (1997): 147–155.